Resolution of Identity Density Functional Theory Augmented with an Empirical Dispersion Term (RI-DFT-D): A Promising Tool for Studying Isolated Small Peptides

Jiří Černý,[†] Petr Jurečka,[‡] Pavel Hobza,[†,‡] and Haydée Valdés*[,†]

Institute of Organic Chemistry and Biochemistry, Academy of Sciences of the Czech Republic and Center for Biomolecules and Complex Molecular Systems, 166 10 Prague 6, Czech Republic, and Department of Physical Chemistry, Palacky University, tr. Svobody 26, 771 46, Olomouc, Czech Republic

Received: October 3, 2006; In Final Form: November 23, 2006

Resolution of identity standard density functional theory augmented with a damped empirical dispersion term (RI-DFT-D) calculations have been carried out on a set of lowest energy minima of tryptophyl−glycine (Trp−Gly) and tryptophyl−glycyl−glycine (Trp−Gly−Gly) peptides. RI-DFT-D (TPSS/TZVP) results are in excellent agreement with benchmark data based on the CCSD(T) method. Experimental spectra could be assigned according to the calculated IR frequencies. Central processing unit (CPU) time requirements are only slightly higher than those needed for the DFT calculations. Consequently, RI-DFT-D theory seems to be a promising methodology for studying oligopeptides with accuracy comparable to ab initio quantum chemical calculations.

1. Introduction

The study of small peptides in the gas phase is a difficult task. Gas-phase spectroscopic techniques,[1,2] though very accurate, suffer from certain limitations (e.g., vibrational spectra do not fully resolve the structure of the systems) and usually, experiments have to be combined with theoretical calculations to provide a complete picture of the system under study. Since ab initio molecular dynamics (MD) simulations for di- and tripeptides are still impractical, the most accurate treatment that can be performed is the combination of semiempirical MD simulations (for an initial screening of the potential energy surface (PES)) followed by quantum chemical calculations carried out on a set of selected (most stable) conformers. Particularly, the combination of MD simulations with quenching (Q) procedures[3] at the approximate self-consistent-charge, density functional tight-binding with empirical dispersion energy (SCC-DFTB-D)[4] level of theory has proven sufficient to localize stable conformations in the PES of small peptides.[5] This theoretical treatment (which adequately covers the London dispersion energy) allows for a semiempirical screening of the PES and thus offers a reliable description of the peptide's conformational landscape. Concerning the quantum chemical calculations, both density functional theory (DFT) and classical correlated ab initio methodologies (e.g., Moller−Plesset perturbation theory) could in principle be applied. An important advantage of DFT methods is their favorable central processing unit (CPU) performance which allows the application of DFT techniques to systems of increasing size and complexity. However, it has been recently shown[6] that DFT should be used with extreme care when studying isolated, small peptides. The reason is that DFT does not provide a proper description of the London dispersion energy between peptide building blocks,[7] which has been proven to play a relevant role in the stability of the conformers that coexist in the gas phase (especially in the case of those systems containing an aromatic side chain). A proper description of the dispersion interaction can be obtained by using correlated ab initio quantum chemical calculations,[5,6] but unfortunately, they are highly computationally demanding, especially for oligopeptides containing more than three amino acids. This is due to the fact that accurate results are only obtained if the CCSD(T) method is applied.[8] A good alternative could be then to use a methodology that will combine both the fast performance of the DFT method, along with a reasonably good description of the dispersion energy. Recently, Jurečka et al. presented a DFT-based method augmented with a damped empirical dispersion term (DFT-D) parametrized for a well-balanced set of 22 van der Waals molecules.[9] As in previous schemes,[4,10] the dispersion energy is described by damped interatomic potentials of the form C_6R^{-6}. The results obtained were in excellent agreement with reference high-level wave function data based on the CCSD(T) method at a considerably lower computational cost. Thus, we decided to test the performance of the above-mentioned methodology for the study of isolated small peptides. Testing this methodology is relevant not only for the study of isolated small peptides itself but also for its potential application to the study of some other relevant biomolecules. We will then compare the energies, geometries, vibrational frequencies, and thermodynamical properties obtained at the DFT-D level of theory with the same properties obtained by means of classical ab initio correlated methods and DFT. In particular, we will study the tryptophyl−glycine (Trp−Gly) and tryptophyl−glycyl−glycine (Trp−Gly−Gly) peptides. We have chosen these systems for two different reasons. On one hand, their relatively small size enables us to carry out high-level correlated ab initio quantum chemical calculations. On the other hand, dispersion energy plays a relevant role in the stabilization of the different conformers coexisting in the gas phase.[6]

2. Theoretical Calculations

2.1. Strategy of Calculation. We have performed resolution of identity (see explanation in section 2.2.2) DFT-D calculations

* To whom correspondence should be addressed. Fax: +420 220 410 320. Tel.: +420 220 410 320. E-mail: haydee.valdes@marge.uochb.cas.cz.
[†] Center for Biomolecules and Complex Molecular Systems.
[‡] Palacky University.

10.1021/jp066504m CCC: $37.00
Published on Web 01/25/2007

on a set of the most stable minima in the PES of the Trp−Gly dipeptide and Trp−Gly−Gly tripeptide as obtained in a previous theoretical study carried out on these systems[6] according to the strategy of calculation described in ref 5. The set of structures considered consists of 15 and 13 conformers for Trp−Gly and Trp−Gly−Gly, respectively. All the calculations have been performed using the TPSS functional[11] as it gives comparable results with those of the B3LYP hybrid functional[12] but at a lower computational cost. Pople 6-311++G(3df,3pd)[13] (abbreviated as LP in this paper) and Ahlrichs TZVP[14] basis sets were used for the geometry optimizations and frequency calculations. Single-point calculations on TPSS/ TZVP geometries were carried out using Dunning's aug-cc-pVQZ[15] with both *g* functions and the most diffuse *f* function removed from the heavy atoms and both *f* functions and the most diffuse *d* function removed from the hydrogen atom (abbreviated as aQZ') and cc-pVTZ[15] basis sets. Harmonic vibrational frequencies were calculated using a numerical Hessian. Different scaling factors were used depending on the type of vibration mode and level of theory employed (see parts a and b of Table 4). All of the scaling factors were obtained as a ratio between the theoretical and experimental frequencies for the Trp−Gly,[6,16] Trp−Gly−Gly,[6,16] and Phe−Gly−Gly[5] set of assigned structures using the least-squares fitting method. The median scaling factor was used to determine zero-point vibrational energies (ZPVE), enthalpies, and entropies. All the thermodynamic properties were calculated under the assumption of the rigid rotor−harmonic oscillator−ideal gas (RR−HO−IG) approximation.

2.2. Computational Methods. *2.2.1. High-level Correlated Ab Initio Quantum Chemical Calculations.* Ab initio quantum chemical calculations have been performed by means of resolution of identity (RI)[17] second-order Moller−Plesset theory (MP2) (see ref 6). RI methods are based on the approximate evaluation of the four-centered two-electron integrals (this computation represents the most demanding part of the calculations) by using three-centered integrals, which are computed considerably faster. As a consequence, the computational time is significantly reduced while at the same time all the electronic integrals are included.

All the conformers here considered were optimized at the RI-MP2/cc-pVTZ level of theory (see ref 6). Total energies (RI-MP2/cc-pVTZ and RI-MP2/cc-pVQZ//RI-MP2/cc-pVTZ) were extrapolated to the complete basis set (CBS) limit using the extrapolation scheme of Helgaker and co-workers.[18] CBS CCSD(T) relative energies were calculated as follows

$$E_{\mathrm{CBS}}{}^{\mathrm{CCSD(T)}} = E_{\mathrm{CBS}}{}^{\mathrm{MP2}} + (E^{\mathrm{CCSD(T)}} - E^{\mathrm{MP2}})|_{\mathrm{smallbasisset}} \quad (1)$$

where the first term represents the CBS limit of the relative MP2 energy and the second term describes the higher-order contributions to the correlation energy (beyond the second perturbation order). The 6-31G*(0.25) basis set has been systematically used for all the present CCSD(T) calculations, as it has been recently shown[19] that, in the case of molecular clusters, it provides satisfactory values of the CCSD(T)-MP2 interaction energy difference. More details about the high-level correlated ab initio quantum chemical calculations can be found in ref 6.

2.2.2. Density Functional Theory Calculations. As it has been already mentioned in the introduction, the major drawback of the DFT theory is its inability to describe properly the London dispersion energy.[20] Thus, DFT theory can provide misleading information in the case of systems where the dispersion energy plays a relevant role (i.e., stacked DNA base pairs or small peptides containing aromatic side chains). More details about the performance of the DFT methodology on isolated small peptides with aromatic side chains can be found in refs 5 and 6. Consequently, for the present study, DFT calculations have been mostly carried out by means of RI-DFT-D methodology.[9] The idea behind this method is very simple: the DFT theory is simply improved by adding an empirical term describing the dispersion energy, while keeping essentially the same CPU time requirements.

In the atomic dispersion scheme, the total dispersion energy is calculated as a sum of all possible pairwise atomic contributions

$$E_{\mathrm{dis}} = -\Sigma_{ij} f_{\mathrm{damp}}(r_{ij}, R^0{}_{ij}) C_{6ij} r_{ij}^{-6} \quad (2)$$

E_{dis} is simply added to the total DFT energy, and the gradient of the dispersion energy is added to the quantum mechanical gradient during the optimization. In eq 2

$$f_{\mathrm{damp}} = 1/(1 + \exp(-d(r_{ij}/(s_{\mathrm{R}} R^0{}_{ij}) - 1)) \quad (3)$$

is a damping function similar to Grimme's damping function[10] to dampen the (otherwise divergent) dispersion interaction at close interatomic distances ($f_{\mathrm{damp}} = 0$) while keeping it unchanged at large distances ($f_{\mathrm{damp}} = 1$), with $d = 35$ for TZVP and aQZ' and $d = 27$ for the LP basis set (both values are taken from ref 9). r_{ij} is the interatomic distance, and s_{R} is a coefficient to scale the van der Waals radii ($s_{\mathrm{R}} = 0.98$ for TZVP, 0.96 for LP, and 0.93 for aQZ'; taken from ref 9). $R^0{}_{ij} = (R^0{}_{ii}{}^3 + R^0{}_{jj}{}^3)/(R^0{}_{ii}{}^2 + R^0{}_{jj}{}^2)$ is the equilibrium van der Waals (vdW) separation derived from the atomic vdW radii,[21] and finally, $C_{6ij} = 2(C_{6ii}{}^2 C_{6jj}{}^2 N_{\mathrm{effi}}\, N_{\mathrm{effj}})^{1/3}/((C_{6ii} N_{\mathrm{effj}}{}^2)^{1/3} + (C_{6jj} N_{\mathrm{effi}}{}^2)^{1/3})$, with N_{eff} being the Slater−Kirkwood effective number of electrons. The values used for these parameters are $C_6 = 0.16$, 1.65, 1.11, and 0.70 J·nm^6·mol^{-1} and $N_{\mathrm{eff}} = 0.80$, 2.5, 2.82, and 3.15 for H, C, N, and O, respectively.[21] The combination rules for $R^0{}_{ij}$ and $C^6{}_{ij}$ were chosen for giving the best results in ref 9.

For one selected conformer, pure RI-DFT[22] (i.e., without empirical dispersion) vibrational frequencies have also been calculated for comparison purposes.

2.3. Codes. Energies, geometries, harmonic vibrational frequencies, and thermodynamic characteristics (RI-MP2, RI-DFT, and RI-DFT-D (our own implementation)) were determined using the TURBOMOLE 5.8 program package.[23] CCSD-(T) calculations were performed with the MOLPRO 2002.6 program.[24]

3. Results and Discussion

3.1. Notation. The performance of the RI-DFT-D methodology has been tested on two sets of structures composed of the 15 and 13 most stable conformers in the PES of Trp−Gly and Trp−Gly−Gly peptides, respectively (see Figures 1 and 2; for the sake of simplicity, we have kept the same nomenclature as that used in ref 6). For the following discussion, we will classify the Trp−Gly dipeptide conformers in two families: H-bonded and non-H-bonded (the names of these latter structures are in italics for easier identification). A more detailed geometrical description of these structures can be found in ref 6. H-bonded refers to structures where the peptide backbone is bent via an $OH_{\mathrm{carb}}\cdots O{=}C_{\mathrm{pep}}$ intramolecular H-bond (e.g., wg01). Non-H-bonded refers to structures with a quite stretched (less bent) peptide backbone extended over the aromatic side chain (e.g., *wg07*). Notice that the notation (non) H-bonded does not refer to a unique intermolecular interaction responsible for the stability

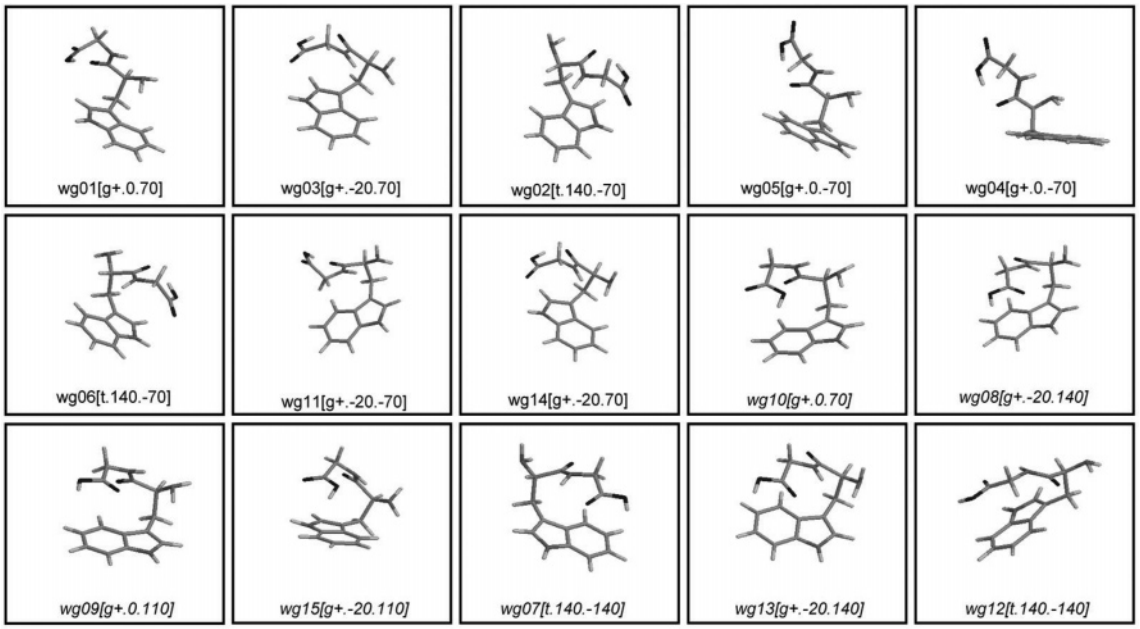

Figure 1. TPSS/TZVP geometries for the 15 most stable structures of Trp−Gly dipeptide. Non-hydrogen -bonded structures are in italics.

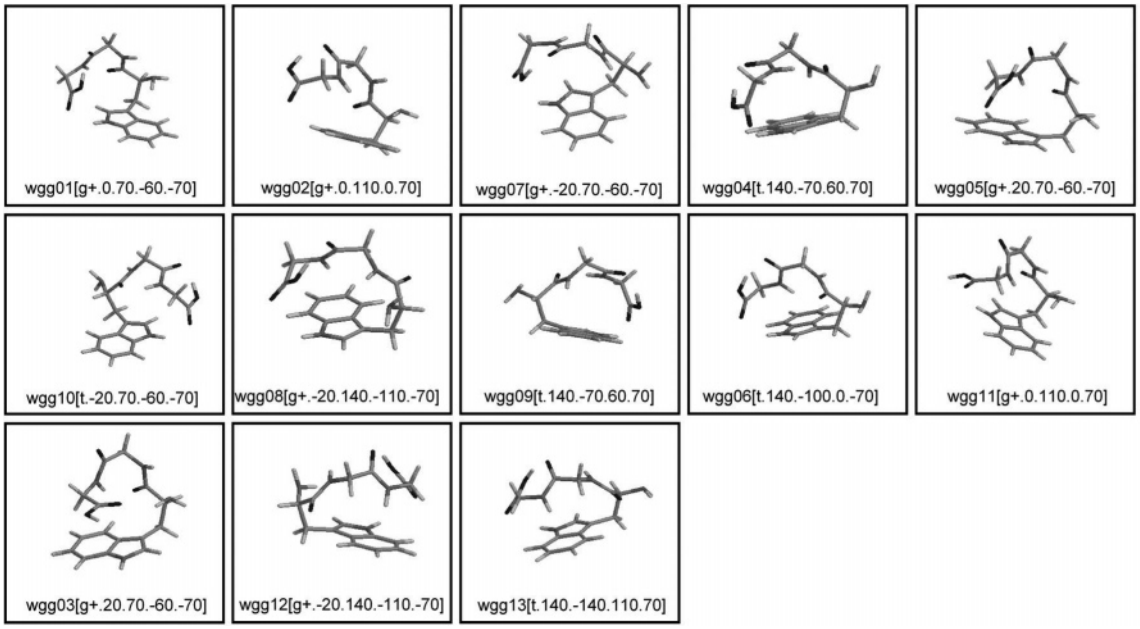

Figure 2. TPSS/TZVP geometries for the 13 most stable structures of the Trp−Gly−Gly tripeptide.

of the system as in the case, for example, of Watson−Crick DNA base pairs. In the present work, all the structures gain approximately the same stability due to the London dispersion forces contribution.[6]

3.1.1. Nomenclature of the Structures. The nomenclature used describes both the order of the conformers according to their enthalpies (H_0) and their peptide backbone geometry described in terms of its principal torsional angles (see Chart 1). The pattern followed for the peptides names is *wgNN*[$\chi_1.\psi_1.\varphi_2$] and *wggNN*[$\chi_1.\psi_1.\varphi_2.\psi_2.\varphi_3$] for Trp−Gly and Trp−Gly−Gly, respectively. *NN* stands for the energetic position of the conformer according to the enthalpy scale. χ_1, ψ_1, φ_2, ψ_2, and φ_3 are the principal torsional angles (see Chart 1). Their possible values (in degrees) are the following: (a) $\chi_1 = 60$ ($g+$), -60 ($g-$), or 180 (t); (b) $\psi_1 = -20$, 0, 20, or 140; (c) $\varphi_2 = -140$, -100, -70, 70, 110, 140; (d) $\psi_2 = -10$, -60, 0, 60, 110, and finally, (e) $\varphi_3 = -70$, 70. A shortcut has been used for the structure names throughout the remaining text.

3.2. Electronic Energies. Parts a and b of Table 1 show the RI-DFT-D relative energies for a set of the most stable conformers in the PES of Trp−Gly and Trp−Gly−Gly peptides, respectively. All the calculations have been performed using the TPSS functional.[11] Basis sets of different qualities and laboratories have been employed. In the case of the Trp−Gly dipeptide (Table 1, part a), H-bonded conformers (first eight entries in the table) are systematically predicted to be more stable than the non-H-bonded ones (remaining entries in part a). The order of structures, as well as the energetic differences among structures, remains almost the same at all levels of theory. For the Trp−Gly−Gly tripeptide (Table 1, part b), similar information is obtained. TPSS/aQZ'//TPSS/TZVP (second column), TPSS/LP//TPSS/TZVP (third column) and TPSS/LP (last col-

CHART 1: Torsional Angles of the Trp−Gly Dipeptide and Trp−Gly−Gly Tripeptide

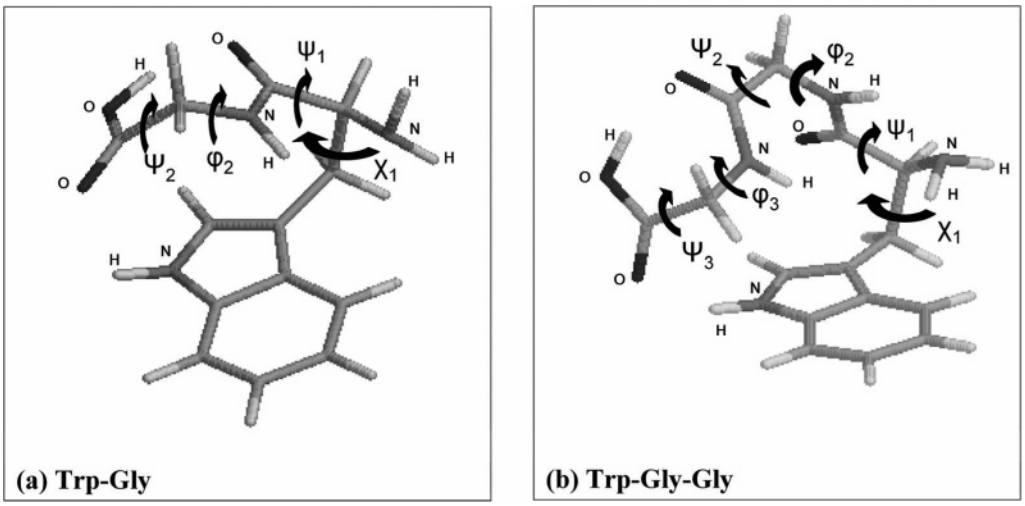

TABLE 1: RI-DFT-D Relative Energies[a] (kcal/mol) for the Most Stable Conformers of Trp−Gly Dipeptide and Trp−Gly−Gly Tripeptide

TPSS/TZVP[b]		TPSS/aQZ'//TPSS/TZVP[c]		TPSS/LP//TPSS/TZVP[d]		TPSS/LP[d]	
			(a) Trp−Gly Dipeptide				
wg01	0.00	wg02	0.00	wg01	0.00	wg01	0.00
wg03	0.51	wg01	0.10	wg03	0.27	wg03	0.24
wg02	1.00	wg03	0.10	wg02	0.36	wg02	0.32
wg05	1.39	wg05	1.00	wg05	1.21	wg06	1.20
wg04	1.43	wg06	1.04	wg06	1.24	wg05	1.21
wg06	1.96	wg04	1.18	wg04	1.44	wg04	1.39
wg11	2.02	wg11	1.33	wg11	1.61	wg11	1.61
wg14	2.75	wg14	1.73	wg14	2.05	wg14	2.05
wg10	*2.98*	*wg08*	*3.29*	*wg08*	*2.96*	*wg08*	*2.89*
wg08	*3.34*	*wg09*	*3.39*	*wg10*	*3.10*	*wg09*	*3.00*
wg09	*3.34*	*wg10*	*3.41*	*wg09*	*3.13*	*wg10*	*3.07*
wg15	*3.35*	*wg07*	*3.47*	*wg07*	*3.24*	*wg07*	*3.23*
wg07	*3.85*	*wg13*	*3.61*	*wg13*	*3.32*	*wg13*	*3.33*
wg13	*4.06*	*wg15*	*3.79*	*wg15*	*3.42*	*wg15*	*3.43*
wg12	*4.50*	*wg12*	*4.01*	*wg12*	*3.68*	*wg12*	*3.71*
			(b) Trp−Gly−Gly Tripeptide				
wgg01	0.00	wgg01	0.00	wgg01	0.00	wgg01	0.00
wgg02	0.49	wgg02	0.72	wgg02	0.34	wgg02	0.28
wgg07	2.35	wgg04	2.19	wgg04	2.21	wgg04	1.98
wgg04	2.87	wgg07	2.24	wgg08	2.47	wgg07	1.99
wgg05	3.27	wgg08	2.70	wgg05	2.68	wgg08	2.47
wgg10	3.32	wgg05	2.84	wgg10	2.95	wgg05	2.71
wgg08	3.54	wgg10	3.01	wgg09	3.09	wgg10	2.91
wgg09	3.83	wgg09	3.19	wgg06	3.24	wgg09	3.01
wgg06	4.00	wgg06	3.52	wgg07	3.46	wgg06	3.23
wgg11	4.46	wgg12	4.44	wgg12	4.21	wgg12	4.20
wgg03	4.80	wgg03	4.99	wgg03	4.34	wgg03	4.29
wgg12	5.84	wgg13	5.07	wgg11	4.76	wgg11	4.69
wgg13	6.27	wgg11	5.19	wgg13	4.78	wgg13	4.85

[a] Energies (1 kcal/mol = 4.184 kJ mol^{-1}) have been evaluated with various basis sets. Structures are labeled according to Figures 1 and 2. Italic font is used to indicate non-H-bonded conformers in part a. [b] Ahlrichs TZVP basis set. [c] Dunning's aug-cc-pVQZ with both *g* functions and the most diffuse *f* function removed from the heavy atoms, and both *f* functions and the most diffuse *d* function removed from the hydrogen atom. [d] Pople 6-311++g(3df,3pd) basis set.

umn) levels of theory give essentially the same order of structures. Concerning the TPSS/TZVP (first column) and TPSS/LP (last column), it might seem, at first sight, that the structures are placed in different positions. However, these discrepancies are not significant since the energetic differences among the structures are really small (e.g., the wgg05, wgg10, and wgg08 case). Finally, it should be noticed that, for both peptides, the energy intervals change when passing from the first (4.50 kcal/mol (18.828 kJ·mol^{-1}, 1 kcal/mol = 4.184 kJ mol^{-1}); 6.27 kcal/mol) to the last column (3.71 kcal/mol; 4.85 kcal/mol). Thus, a higher energetic cutoff has to be considered at the inferior level of theory to select the same number of conformers. The proper selection of conformers is particularly important when having to predict which conformers will be observed experimentally. From analysis of both parts, it seems clear that the TPSS/TZVP level of theory (first column in parts a and b of Table 1) gives similar information compared with the higher level calculations (second, third, and last columns in parts a and b of Table 1) at a lower computational cost. This is relevant since the study of larger systems requires methodologies offering a good compromise between accuracy and reasonable CPU time requirements.

TABLE 2: Relatives Energies (in kcal/mol; 1 kcal/mol = 4.184 kJ mol^{-1}) Calculated for the Most Stable Conformers of Trp−Gly Dipeptide and Trp−Gly−Gly Tripeptide[a] Using Different Methodologies

RI-DFT-D[b]		RI-MP2[c]		RI-MP2[d]		$E_{CBS}^{CCSD(T)}$[e]	
			(a) Trp−Gly Dipeptide				
wg01	0.00	wg03	0.00	wg01	0.00	wg01	0.00
wg03	0.51	wg02	0.00	wg02	0.00	wg02	0.42
wg02	1.00	wg01	0.11	wg03	0.53	wg03	1.03
wg05	1.39	*wg08*	*0.70*	*wg09*	*0.66*	wg05	1.23
wg04	1.43	*wg09*	*0.92*	*wg08*	*0.78*	wg04	1.24
wg06	1.96	wg06	0.97	wg06	0.92	wg06	1.32
wg11	2.02	*wg13*	*1.27*	*wg07*	*1.10*	*wg09*	*2.15*
wg14	2.75	*wg15*	*1.29*	wg05	1.10	wg11	2.26
wg10	*2.98*	*wg07*	*1.30*	*wg13*	*1.17*	*wg07*	*2.27*
wg08	*3.34*	wg05	1.59	*wg10*	*1.37*	*wg08*	*2.34*
wg09	*3.34*	*wg10*	*1.66*	wg04	1.47	*wg10*	*2.40*
wg15	*3.35*	wg14	1.86	*wg12*	*1.60*	wg14	2.43
wg07	*3.85*	wg11	1.90	wg11	1.65	*wg13*	*2.71*
wg13	*4.06*	wg04	1.93	*wg15*	*1.77*	*wg12*	*2.84*
wg12	*4.50*	*wg12*	*1.95*	wg14	1.98	*wg15*	*3.04*
			(b) Trp−Gly−Gly Tripeptide				
wgg01	0.00	wgg02	0.00	wgg02	0.00	wgg01	0.00
wgg02	0.49	wgg01	0.16	wgg01	0.47	wgg02	0.42
wgg07	2.35	wgg08	0.99	wgg08	1.51	wgg04	2.24
wgg04	2.87	wgg03	1.55	wgg03	1.57	wgg05	2.27
wgg05	3.27	wgg07	1.86	wgg05	2.09	wgg03	2.32
wgg10	3.32	wgg04	1.93	wgg04	2.28	wgg07	2.75
wgg08	3.54	wgg05	2.09	wgg06	2.68	wgg08	2.85
wgg09	3.83	wgg12	2.61	wgg07	2.70	wgg09	3.05
wgg06	4.00	wgg09	2.84	wgg12	2.90	wgg06	3.06
wgg11	4.46	wgg06	3.05	wgg11	3.04	wgg10	3.38
wgg03	4.80	wgg11	3.19	wgg09	3.14	wgg11	4.04
wgg12	5.84	wgg13	3.48	wgg13	3.58	wgg12	4.19
wgg13	6.27	wgg10	3.50	wgg10	3.66	wgg13	4.55

[a] Structures are labeled according to Figures 1 and 2. Italic font is used to indicate non-H-bonded conformers in part a. [b] TPSS/TZVP. [c] RI-MP2/cc-pVTZ optimization energies (see ref 6). [d] RI-MP2/CBS energies calculated on RI-MP2/cc-pVTZ optimized geometries (see ref 6). [e] Total relative energy evaluated as a sum of CBS RI-MP2 relative energy and a difference between CCSD(T) and MP2 relative energies.

Parts a and b in Table 2 show the performance of the RI-DFT-D methodology compared with the RI-MP2 and the CCSD(T) methods for the Trp−Gly and Trp−Gly−Gly peptides. For the sake of simplicity (see discussion about parts a and b in Table 1), only TPSS/TZVP relative energies have been included. Mean absolute deviations (MAD) between the RI-DFT-D and the RI-MP2 and CCSD(T) methods can be found in Tables A and B in the Supporting information. Three observations can be made from a detailed analysis of the data collected in Table 2, part a. First, the RI-DFT-D (TPSS/TZVP) and the CCSD(T) methods predict the H-bonded conformers to be lower in energy than the non-H-bonded ones whereas, according to the RI-MP2 calculations (with the cc-pVTZ basis set (second column) and with a complete basis set (third column)), H-bonded and non-H-bonded structures are interchanged. Second, the overall performance of the RI-DFT-D and RI-MP2 methods is comparable (see values of the average of MAD in Tables A and B in the Supporting Information). Third, the relative energies calculated by the means of the MP2 method are systematically smaller than the CCSD(T)/CBS, whereas the RI-DFT-D relative energies are larger. This deviation is particularly noticeable in the case of the non-H-bonded structures. The above-mentioned differences can be understood in terms of the description provided by the MP2 and DFT-D methodologies of the dispersion energy. On one hand, the *extra* stability predicted by the MP2 method is in agreement with the fact that MP2 overestimates the binding in the dispersion bond systems.[25,26] Notice that the basis set size effect on the MP2 order of energies can be disregarded since RI-MP2/CBS and RI-MP2/cc-pVTZ levels of theory provide very similar information. On the other hand, from the comparison between the RI-DFT-D and CCSD(T) energies, it seems clear that the RI-DFT-D method slightly underestimates the dispersion energy contribution. Finally, the intramolecular basis set superposition error (BSSE) effect cannot be, in principle, disregarded.[27,28] However, CCSD(T)/CBS and MP2/CBS energies are, practically, BSSE-free, and the RI-DFT-D relative energies are not expected to be largely influenced by the intramolecular BSSE, since it is comparatively smaller than for wave function theory calculations and it is partly compensated by the empirical dispersion parametrization.[9] In the case of the Trp−Gly−Gly tripeptide (Table 2, part b), similar observations and conclusions can be made. TPSS/TZVP relative energies are comparable to the CCSD(T)/CBS ones, with the largest [CCSD(T)−RI-DFT-D] difference being ∼2.5 kcal/mol (wgg03) and the smallest ∼0.06 kcal/mol (wgg10). Structures collected in part b of Table 2 lie within a smaller energy interval at the RI-MP2/CBS (also RI-MP2/cc-pVTZ) (∼3.5 kcal/mol) level of theory than the CCSD-(T)/CBS ones, whereas at the TPSS/TZVP level of theory, the energy interval is larger (∼6.0 kcal/mol). These results can be again justified in terms of the *incomplete* description of the dispersion energy (see above) given by the RI-MP2 (overestimation) and the RI-DFT-D (underestimation) methodologies. From the data collected in parts a and b in Table 2, it can be concluded that the TPSS/TZVP level of theory gives comparable information to the CCSD(T)/CBS level but at a considerably lower computational cost. This is an important result since it reveals the RI-DFT-D methodology as a promising tool for studying larger interesting biological systems as an alternative to the prohibitive (for these systems) classical correlated ab initio methodologies.

3.3. Frequencies. The empirical dispersion correction is meant as a long-range correction, that is, it is not supposed to affect the strength of bonding of the neighboring atoms. Ideally,

TABLE 3: Comparison of Chosen Vibrational Modes (cm^{-1}) of *wg09* Calculated by Pure DFT (TPSS/TZVP), DFT-D (TPSS/TZVP), and MP2/cc-pVDZ Methods[a]

mode[b]		RI-DFT	RI-DFT-D	RI-MP2
ν_1		21[c]	31	31
ν_2		39[c]	57	50
ν_3		46[c]	70	68
ν_4	structure opening	61[c]	54	82
ν_5		79[c]	82	89
ν_6		92[c]	113	98
ν_{11}	peptide backbone bend	208	212	228
ν_{20}	indole in-plane bend	455	457	460
ν_{36}	indole ring "breathing"	758	761	767
ν_{45}	NH_2 out-of-plane	909	913	946
ν_{68}	comb. CH_2COOH bend	1377	1374	1435
ν_{75}	NH peptide bend	1505	1516	1565
ν_{80}	CO peptide stretch	1682	1684	1780
ν_{86}	CH_2 antisymm. stretch	3058	3066	3181
ν_{96}	OH stretch	3643	3647	3759

[a] All frequencies in this table are unscaled. [b] MP2 order. [c] Pure DFT modes do not correspond to the MP2 modes, the structures are too different.

stretching frequencies calculated by pure DFT should remain almost unaffected in DFT-D. On the other hand, the low-frequency modes of larger molecules are co-determined by interactions of distant parts of the molecule with possible significant attractive dispersion contribution; therefore, we would expect some shift toward higher frequencies for them. The remaining vibrational modes, which lie energetically in between stretches and low modes, like bending, could also be partially affected by the additional dispersion in DFT-D; however, there is no study that would indicate the extent of this effect.

The first guess on the magnitude of the dispersion contribution (within our approach) can be obtained by extracting the pairwise dispersion energy contribution to the 1−2, 1−3 (over two bonds), and 1−4 (over three bonds) interactions in a molecule. For instance, the 1−2 contribution for the *wg09* molecule is on average 3×10^{-6} kcal/mol per bond, that is, it is clearly negligible. The same holds for the 1−3 interactions, where it is 2×10^{-3} kcal/mol. This is a consequence of the relatively steep damping function we use to reduce the dispersion interaction at short distances. However, in the case of the 1−4 interactions, the average dispersion contribution is already about 0.1 kcal/mol, which means that the respective bending modes can be somewhat affected. In total, the sum of all 1−4 interactions makes about half of the total intramolecular dispersion energy in the *wg09* molecule, −7.2 kcal/ mol out of −13.7 kcal/mol. A relatively high dispersion contribution to the 1−4 interactions is rather surprising, and further investigation will be needed to find out if this picture is realistic or if it is an artifact of the DFT-D method. At the moment, we will rely on the DFT-D parametrization as it is and we will test it further by direct comparison of the vibrational frequencies calculated by different QM methods.

Table 3 compares a few vibrational modes of *wg09* calculated by pure DFT (TPSS/ TZVP), DFT-D (TPSS/TZVP), and MP2/ cc-pVDZ methods. (The *wg09* structure was chosen rather arbitrarily except that we required that it is compact and exhibits a distinct structure opening mode.) In addition to the six lowest modes, we have chosen also six bending and three stretching modes by random, except that we limited ourselves to the well-localized vibrations that can be easily identified for all three methods. All frequencies considered are unscaled. Let us first have a look at the lowest vibrations, which are traditionally treated separately, for example, by using different scaling factors. Comparing the last three columns in Table 3, we can see that

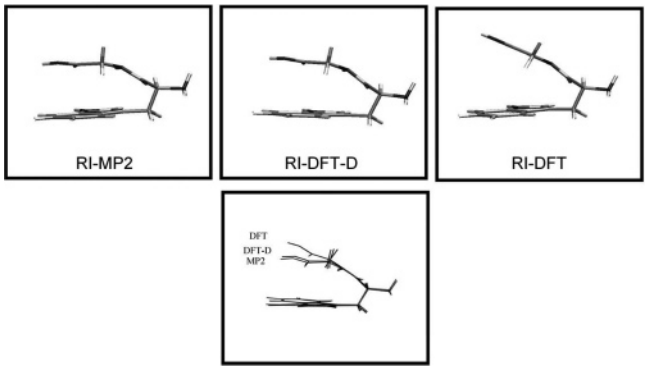

Figure 3. Comparison of the description of the London dispersion forces provided by the DFT-D, MP2, and DFT methodologies. The alignment between the MP2, DFT-D, and DFT-optimized geometries is also included.

the DFT-D frequencies are quite close to the MP2 results, while the pure DFT results are in error, as a consequence of a somewhat more opened DFT geometry (see Figure 3) (pure DFT vibrational modes could not be matched with the MP2 modes). The only larger DFT-D deviation is seen for the ν_4 mode, which is much lower in DFT-D than in MP2. However, this discrepancy can easily be traced to the overestimated dispersion in MP2, which is most likely to affect the ν_4 mode, corresponding to the opening of the closed structure, the compactness of which is preserved mainly by dispersion (optimization in pure DFT leads to full opening). We can conclude that DFT-D reproduces the low-energy MP2 vibrational pattern reasonably well, correcting for the well-known MP2 dispersion overestimation, while pure DFT fails here.

Regarding the higher frequency modes, like bending (ν_{11}−ν_{75} in Table 3) and stretching modes (ν_{80}−ν_{96} in Table 3) the pure DFT methods are known to give smaller standard deviations than the MP2 method and also scaling factors closer to 1.0.[29] For practical purposes, this is widely considered an advantage of DFT over MP2, and we will adopt this viewpoint here (this favorable picture could, however, change if we considered the anharmonicity effects). Here, the additional empirical dispersion in DFT-D shifts the DFT frequencies toward the MP2 ones, but only slightly, the higher the frequency the smaller the (relative) shift (on average), preserving the behavior of the pure DFT method. The highest stretches are shifted by a few reciprocal centimeters, that is, much more than we would expect from the 1−2 dispersion contribution (see above), which could be explained by the quite different equilibrium structure. The DFT-D method thus inherits as good of a description of the high-frequency modes as of DFT and improves the low-frequency modes considerably.

Parts a and b of Table 4 collect the (unscaled and scaled) RI-DFT-D (TPSS/TZVP and TPSS/LP) mid (3100−3600 and 1100−1800 cm^{-1}) IR frequencies for the experimentally observed conformers of the Trp−Gly and Trp−Gly−Gly peptides, respectively.[6] Experimental frequencies are also included.[16,30] The 3100−3600 cm^{-1} spectral region shows three lines of absorption corresponding to the carboxyl O−H stretching (OH), the indole N−H stretching (NH_{ind}), and the peptide N−H stretching (NH_{pep}) vibrations. The four bands observed in the 1100−1800 cm^{-1} spectral region can be assigned to the carbonyl of the carboxyl group and carbonyl peptide stretching vibrations (CO_{carb} and CO_{pep}, respectively), the peptide N−H in-plane bending vibration (NH_{ipb}), and to the carboxyl O−H in-plane bending vibration (OH_{ipb}). RI-MP2/cc-pVDZ frequencies[6] have also been included for comparison purposes. The

TABLE 4: Experimental and RI-DFT-D Scaled Vibrational Frequencies (cm^{-1}) for the Experimentally Observed Conformers of Trp−Gly Dipeptide and Trp−Gly−Gly Tripeptide[a]

(a) Trp−Gly Dipeptide

conformer	OH[b]	NH_{ind}[c]	NH_{pep}[d]	CO_{carb}[b]	CO_{pep}[b]	NH_{ipb}[b]	OH_{ipb}[b]
d	3598	3522	3407				
wg08	3595	3524	3405	1734	1665	1483	1123
	[3650]	[3614]	[3443]	[1760]	[1691]	[1506]	[1140]
(LP)	3596	3529	3407	1731	1661	1468	1120
	[3654]	[3616]	[3448]	[1759]	[1688]	[1492]	[1138]
RI-MP2/cc-pVDZ	3599	3528	3391	1760	1706	1485	1133
	[3765]	[3683]	[3566]	[1841]	[1785]	[1553]	[1185]
b	3582	3522	3412	1789	1705	1516	1106
wg09	3592	3525	3423	1729	1656	1467	1122
	[3647]	[3615]	[3461]	[1758]	[1682]	[1492]	[1140]
(LP)	3596	3527	3435	1737	1656	1486	1113
	[3652]	[3614]	[3477]	[1757]	[1683]	[1491]	[1140]
RI-MP2/cc-pVDZ	3598	3528	3416	1758	1695	1480	1142
	[3764]	[3683]	[3592]	[1839]	[1773]	[1548]	[1195]
a	3588	3519	3422	1794	1705	1502	1129
wg07	3594	3523	3444	1731	1656	1470	1123
	[3649]	[3613]	[3482]	[1767]	[1684]	[1516]	[1131]
(LP)	3594	3528	3442	1741	1658	1493	1114
	[3652]	[3615]	[3484]	[1765]	[1683]	[1510]	[1130]
RI-MP2/cc-pVDZ	3594	3527	3432	1762	1701	1496	1131
	[3759]	[3682]	[3609]	[1843]	[1779]	[1565]	[1183]

(b) Trp−Gly−Gly Tripeptide

conformer	OH[b]	NH_{ind}[c]	NH_{pep1}[d]	NH_{pep2}[d]	CO_{carb}[b]	CO_{pep1}[b]	CO_{pep2}[b]	NH_{ipb2}[b]	NH_{ipb1}[b]	OH_{ipb}[b]
a		3381	3419	3431	1771	1671[e]	(????)[e]	1551	1504	1421
wgg02	3058	3352	3469	3404	1724	1672	1617	1504	1476	1395
	[3105]	[3445]	[3493]	[3429]	[1750]	[1697]	[1642]	[1526]	[1498]	[1417]
(LP)	3033	3347	3452	3403	1722	1669	1613	1501	1469	1409
	[3082]	[3429]	[3494]	[3404]	[1748]	[1695]	[1639]	[1524]	[1492]	[1431]
RI-MP2/cc-pVDZ	3208	3352	3411	3431	1746	1709	1662	1510	1477	1420
	[3356]	[3499]	[3587]	[3608]	[1826]	[1788]	[1738]	[1579]	[1545]	[1485]
b	3585	3520	3396	3388	1782	1716	1681	1510[e]	(????)[e]	1106
wgg03	3595	3523	3424	3403	1734	1680	1641	1501	1486	1078
	[3650]	[3613]	[3462]	[3441]	[1760]	[1705]	[1666]	[1523]	[1509]	[1094]
(LP)	3595	3527	3405	3413	1731	1678	1637	1497	1483	1080
	[3653]	[3614]	[3454]	[3446]	[1758]	[1704]	[1662]	[1520]	[1506]	[1097]
RI-MP2/cc-pVDZ	3600	3524	3408	3394	1761	1715	1679	1498[e]	(1480)[e]	1110
	[3766]	[3678]	[3584]	[3569]	[1842]	[1794]	[1756]	[1567]	[1548]	[1161]

[a] Frequencies have been calculated at the TPSS/TZVP and TPSS/LP levels of theory. RI-MP2/cc-pVDZ frequencies have been added for comparison purposes (see ref 6). In part a, labels a, b, and d are the names of the experimental structures (see refs 16 and 30). Italic font is used to indicate non-H-bonded conformers. Unscaled frequency values are in brackets. [b] The scaling factor for the OH frequency and for all the mid-IR bands was set at 0.985 (TPSS/TZVP), 0.984 (TPSS/LP), and 0.956 (MP2/cc-pVDZ). [c] The scaling factor for NH_{ind} frequency was set at 0.975 (TPSS/TZVP), 0.976 (TPSS/LP), and 0.958 (MP2/cc-pVDZ). [d] The scaling factor for NH_{pep} frequency was set at 0.989 (TPSS/TZVP), 0.988 (TPSS/LP), and 0.951 (MP2/cc-pVDZ). [e] Neighboring vibration modes are coupled; the band with the value in parentheses has marginal intensities; (????) means that the experimental value of the coupled vibration mode with marginal intensity was impossible to measure.

results collected in Table 4 are very satisfactory. To start with, TPSS/TZVP frequencies are similar to the ones obtained with the larger (LP) basis set but at a lower computational cost, suggesting that the TPSS/TZVP level of theory can be recommended for frequency calculation of medium-sized systems. Second, DFT-D scaling factors are, as expected,[29] close to unity and larger than the MP2 ones, implying the following: (a) that they could be, in principle, used without scaling and (b) that DFT-D performs better (even without using scaling factors) than MP2. Finally, there is a nice agreement between the RI-DFT-D theoretical frequencies and the experimental ones. Thus, it is possible to assign (at least qualitatively) the experimental spectra according to the RI-DFT-D frequencies (see a more detailed discussion about the assignment of the spectra in ref 6). For instance, in the case of the Trp−Gly dipeptide, the red shifting observed in the NH_{pep} stretching vibration frequencies (νNH_{pep}) (free νNH_{pep} in *N*-acetyl tryptophan methyl amide (NATMA) ranges between 3454 and 3466 cm^{-1} depending on the conformer[31]) is well reproduced at the TPSS/TZVP theoretical level.

3.4. Thermodynamic Properties. Parts a and b in Table 5 contain TPSS/TZVP relative enthalpies and relative Gibbs energies for the most stable conformers of the Trp−Gly and Trp−Gly−Gly peptides. Relative populations assuming a Maxwell−Boltzmann (M−B) distribution at 300 K are also included (see the last column in Table 5). Similar distributions were observed at different temperatures (T = 10, 100, 400, and 500 K). TPSS/LP thermodynamic properties can be found in the Supporting Information (Tables C and D). Frequencies scaled with a single scaling factor (the OH scaling factor; 0.985 for TPSS/TZVP and 0.984 for TPSS/LP) were systematically used for all the thermodynamic calculations.

From a detailed analysis of Table 5, it can be concluded that the inclusion of vibrational contributions to the internal thermal energy decreases the energetic interval by approximately 1 kcal/mol (see the first column in Table 2 and first column in Table 5), but it does not practically affect the order of structures. However, the structures are placed in totally different positions according to the Gibbs energy scale (fourth column), suggesting that entropic contributions play an important role in the stability

TABLE 5: RI-DFT-D (TPSS/TZVP) Relative Enthalpies and Gibbs Energies (in kcal/mol; 1 kcal/mol = 4.184 kJ mol^{-1}) for the Most Stable Conformers of Trp−Gly Dipeptide and Trp−Gly−Gly Tripeptide[a]

	ΔH		ΔG	Pop
	(a) Trp−Gly Dipeptide			
wg01	0.00	wg01	0.00	450
wg03	0.58	wg04	0.47	206
wg02	0.87	wg05	0.86	106
wg05	1.15	wg02	1.16	65
wg04	1.23	wg03	1.28	52
wg06	1.83	*wg08*	*1.66*	*28*
wg11	2.08	*wg09*	*1.76*	*24*
wg10	*2.53*	*wg07*	*1.86*	*20*
wg09	*2.59*	*wg10*	*2.03*	*15*
wg14	2.63	wg11	2.08	14
wg08	*2.76*	wg06	2.24	10
wg07	*2.95*	*wg12*	*2.79*	*4*
wg15	*2.97*	wg14	2.92	3
wg13	*3.60*	*wg15*	*3.08*	*3*
wg12	*3.65*	*wg13*	*3.41*	*1*
	(b) Trp−Gly−Gly Tripeptide			
wgg01	0.00	wgg01	0.00	509
wgg02	0.42	wgg02	0.28	316
wgg07	2.05	wgg04	1.39	49
wgg04	2.37	wgg07	1.68	30
wgg10	2.79	wgg11	1.86	22
wgg05	2.97	wgg10	2.11	15
wgg08	3.19	wgg09	2.15	14
wgg09	3.29	wgg05	2.29	11
wgg06	3.57	wgg06	2.59	7
wgg11	3.82	wgg08	2.85	4
wgg03	4.11	wgg03	2.92	4
wgg12	5.30	wgg13	4.73	0
wgg13	5.52	wgg12	4.84	0

[a] The population of the structures was calculated assuming a Maxwell-Boltzman distribution of 300 K. The enthalpies and Gibbs energies were calculated assuming a scaling factor equal to 0.985. Italic font is used to indicate non-H-bonded conformers.

of the conformers in the free energy surface (FES). For instance, in the case of the Trp−Gly dipeptide (Table 5, part a), the position of the experimentally observed structures (*wg08*, *wg09*, and *wg07*) changes from 10th, 11th, and 13th (in the PES) to 6th, 7th, and 8th (in the FES). Here, it should be mentioned that no Gibbs energies (neither populations) have been evaluated by means of MD simulations. The reason is simply that frequently used empirical force fields (e.g., AMBER, CHARMM) are not recommended for a study of this type of system.[5] Regarding the MD simulations at the SCC-DFTB-D level of theory, longer trajectories should be run to obtain reliable values of the thermodynamic properties. Notice that the MD/Q SCC-DFTB-D simulations are only done with the purpose of scanning the PES for localizing all the possible exiting minima, which requires shorter runs. A striking result derived from the populations collected in Table 5 is that the most populated structures do not correspond with the ones observed experimentally (see assignment of the spectra above and in ref 6). There are, though, a few different reasons for this. Starting with the experimental data, it can occur that the complexity of the spectra hinders extraction of some of the information that, on the other hand, can easily be obtained theoretically (see a more detailed discussion in ref 6). But still, a major source of this disagreement is without a doubt due to the fact that frequencies are calculated in the context of the RR-HO-IG approximation. Especially critical is the calculation of the low-frequency vibrations which contribute dominantly to the vibrational entropy. In general, the optimum scaling factor for low-frequency vibrations is not the same as the standard value for the particular method[29] and, what is more, it is questionable if any theoretically sound scaling factor can be found at all. Also, to our knowledge, no experimental frequencies below 800 cm^{-1} are available for the systems under study (or similar), and thus, for the sake of simplicity we used the same scaling factor for both high and low-frequency vibrations. In principle, more accurate frequencies could be obtained including anharmonicity effects. However, in a previous study carried out on a guanine−cytosine complex with an enolic structure,[32] it was shown that anharmonic and harmonic frequencies did not substantially differ, whereas the anharmonic frequencies are computationally more demanding. Yet, it would be very interesting to study the effect of anharmonicity in the calculation of ZPVE, enthalpies and entropies in the case of isolated small peptides. Finally, the population analysis calculated according to the M−B distribution is also a subject of discussion since again is based on the RR-HO-IG approximation. However, although the RR-HO-IG approximation could bring some uncertainty to our calculations and, consequently, the relative order of the conformers could be slightly changed, the relative proportions of conformer populations in the thermodynamic equilibrium should still be reliable.[33] Thus, according to theoretical calculations, it seems that there are more conformers coexisting in the gas phase than those observed experimentally. This is in agreement with the above-mentioned possibility that the experimental spectrum could possibly not be fully resolved yet (see a more detailed discussion in ref 6).

3.5. Geometries. TPSS/TZVP optimized geometries of the most stable conformers of Trp−Gly and Trp−Gly−Gly are collected in Figures 1 and 2, respectively. TPSS/LP structural information can be found in the Supporting information (Figures 1 and 2). MP2/ cc-pVTZ geometries[6] were used as the initial structures for the DFT-D optimization. The same number of minima was found in both the MP2 and RI-DFT-D PES. Notice, however, that this was not the case when using standard DFT methodology,[6] that is, the number of minima found in the DFT level is inferior (in two structures), suggesting that the use of a methodology that properly covers the dispersion energy is essential for the study of these systems. A more detailed discussion about the performance of the DFT-D method for geometry optimizations can be found in ref 9. There, it was concluded that DFT-D geometries obtained by full gradient optimization are in good agreement with reference geometries obtained either by means of CCSD(T) numerical gradient optimization or (depending on the size of the system) by means of MP2 counterpoise corrected optimizations with analytical gradients. In agreement with these results, the root mean square (rms) found when comparing DFT-D (TPSS/TZVP or TPSS/LP) with MP2 (MP2/cc-pVTZ) structures is rather small (see Tables E and F in the Supporting Information). Unfortunately, CCSD(T) geometry optimizations are prohibitive for the present systems. A more detailed discussion about the geometrical features of Trp−Gly and Trp−Gly−Gly can also be found in ref 6.

A final comment should be made on the influence of the London dispersion forces in the geometry of small peptides. Figure 3 nicely illustrates the description given by the DFT-D, MP2, and DFT methodologies of such forces and it allows for a qualitative comparison between them. In agreement with the trends found in the electronic energies (explained in terms of over- and underestimation of the dispersion forces by MP2 and DFT-D, respectively), the distance between the peptide backbone and the aromatic side chain is slightly shorter in the MP2 structure than in the DFT-D conformer (see the overlap of the

structures in Figure 3). From Figure 3, it is also clear that the DFT methodology can provide a completely wrong picture of the geometry of the system (see discussion in ref 6).

4. Conclusions

An overall conclusion from the present work is that the DFT-D method provides results comparable with those obtained by means of more sophisticated ab initio quantum chemical calculations (i.e., CCSD(T)/CBS) at a considerably lower computational cost. Regarding vibrational frequencies, it substantially improves description of low-frequency modes, while keeping the relatively good performance of pure DFT for higher frequencies. Another important point is that, even when the DFT-D scheme is clearly superior to the standard density functionals, their CPU time requirements are almost the same. The comparison with experimental results is also satisfactory. In general, the RI-DFT-D method provides enough reliable information as to allow for the assignment of the experimental IR spectra. Then, the DFT-D method should be considered as a possible candidate when studying isolated small and medium-sized peptides. The reason is 3-fold: (a) it provides reasonably accurate results while the CPU time consumed is still affordable, (b) DFT-D calculations can be very helpful for obtaining some directions and insights into possible improvements of the currently used empirical potentials, and (c) it can be used as a preliminary step to obtain input geometries that can be used later for further calculations at higher levels of theory, like CCSD(T).

Acknowledgment. This work has been part of the research project Z4 055 905 and it was supported by grants from the Grant Agency of the Academy of Sciences of the Czech Republic (Grant No. A400550510) and Ministry of Education of the Czech Republic (Center for Biomolecules and Complex Molecular Systems, LC512) and National Science Foundation under Contract No. CHE-0244341. It was supported also by Grant No. MSM6198959216 (P.J.) from the MSMT of the Czech Republic.

Supporting Information Available: Mean absolute deviation between the RI-DFT-D method and the RI-MP2 and CCSD(T) methods (Tables A and B); TPSS/LP relative enthalpies and Gibbs energies for the most stable conformers of Trp−Gly and Trp−Gly−Gly peptides (Tables C and D); rms values obtained from the comparison between TPSS/TZVP or TPSS/LP and MP2/cc-PVTZ geometries (Tables E and F); and TPSS/LP structural information (Figures 1 and 2) are given. This material is available free of charge via the Internet at http://pubs.acs.org.

References and Notes

(1) Nir, E.; Plützer, Ch.; Kleinermanns, K.; de Vries, M. *Eur. Phys. J. D* **2002**, *20*, 317−329.

(2) Lesarri, A.; Mata, S.; Lopez, J. C.; Alonso, J. L. *Rev. Sci. Instrum.* **2003**, *74*, 4799−4804.

(3) Ryjáček, F.; Engkwist, O.; Vacek, J.; Kratochvíl, M.; Hobza, P. *J. Phys. Chem. A* **2001**, *105*, 1197−1202.

(4) Elstner, M.; Hobza, P.; Frauenheim, T.; Suhai, S.; Kaxiras, E. *J. Chem. Phys.* **2001**, *114*, 5149−5155.

(5) Řeha, D.; Valdés, H.; Vondrášek, J.; Hobza, P.; Abu-Riziq, A.; Crews, B.; de Vries, M. S. *Chem. Eur. J.* **2005**, *11*, 6803−6817.

(6) Valdés, H.; Řeha, D.; Hobza, P. *J. Phys. Chem. B* **2006**, *110*, 6385−6396.

(7) Dabkowska, I.; Valdés-González, H.; Jurečka, P.; Hobza, P. *J. Phys. Chem. A* **2005**, *109*, 1131−1136.

(8) Šponer, J.; Hobza, P. *Collect. Czech. Chem. Commun.* **2003**, *68*, 2231−2282.

(9) Jurečka, P.; Černý, J.; Hobza, P.; Salahub, D. R. *J. Comput. Chem.*, in press.

(10) (a) Grimme, S. *J. Comput. Chem.* **2004**, *25*, 1463−1473. (b) Grimme, S. *J. Comput. Chem.* **2006**, *27*, 1787−1799.

(11) Tao, J.; Perdew, J. P.; Staroverov, V. N.; Scuseria, G. E. *Phys. Rev. Lett.* **2003**, *91*, 146401.

(12) Becke, A. D. *Phys. Rev. A* **1988**, *38*, 3098−3100.

(13) (a) Krishnan, R.; Binkley, J. S.; Seeger, R.; Pople, J. A. *J. Chem. Phys.* **1980**, *72*, 650−654. (b) Clark, T.; Chandrasekhar, J.; Spitznagel, G. W.; Schleyer, P. von R. *J. Comput. Chem.* **1983**, *4*, 294−301. (c) Gill, P. M. W.; Johnson, B. G.; Pople, J. A.; Frisch, M. J. *Chem. Phys. Lett.* **1992**, *197*, 499−505. (d) Frisch, M. J.; Pople, J. A.; Binkley, J. S. *J. Chem. Phys.* **1984**, *80*, 3265−3269.

(14) Schäfer, A.; Huber, C.; Ahlrichs, R. *J. Chem. Phys.* **1994**, *100*, 5829−5835.

(15) (a) Dunning, T. H., Jr. *J. Chem. Phys.* **1989**, *90*, 1007−1023. (b) Kendall, R. A.; Dunning, T. H., Jr.; Harrison, R. J. *J. Chem. Phys.* **1992**, *96*, 6796−6806.

(16) Bakker, J. M.; Plützer, C.; Hünig, I.; Häber, T.; Compagnon, I.; Helden, G. Von Meijer, G.; Kleinermanns, K. *ChemPhysChem* **2005**, *6*, 120−128.

(17) Feyereisen, M.; Fitzgerald, G.; Komornicki, A. *Chem. Phys. Lett.* **1993**, *208*, 359−363.

(18) Halkier, A.; Helgaker, T.; Jørgensen, P.; Klopper, W.; Koch, H.; Olsen, J.; Wilson, A. K. *Chem. Phys. Lett.* **1998**, *286*, 243−252.

(19) Hobza, P.; Šponer, J. *J. Am. Chem. Soc.* **2002**, *124*, 11802−11808.

(20) Šponer, J.; Leszczynski, J.; Hobza, P. *J. Comput. Chem.* **1996**, *17*, 841−850.

(21) Halgren, T. A. *J. Am. Chem. Soc.* **1992**, *114*, 7827−7843.

(22) Kendall, R. A.; Früchtl, H. A. *Theor. Chem. Acc.* **1997**, *97*, 158−163.

(23) Ahlrichs, R.; Bär, M.; Häser, M.; Horn, H.; Kölmel, C. *Chem. Phys. Lett.* **1989**, *162*, 165−169.

(24) *MOLPRO*, a package of *ab initio* programs designed by Werner, H.-J. and Knowles, P. J., version 2002.1, Amos, R. D.; Bernhardsson, A.; Berning, A.; Celani, P.; Cooper, D. L.; Deegan, M. J. O.; Dobbyn, A. J.; Eckert, F.; Hampel, C.; Hetzer, G.; Knowles, P. J.; Korona, T.; Lindh, R.; Lloyd, A. W.; McNicholas, S. J.; Manby, F. R.; Meyer, W.; Mura, M. E.; Nicklaβ, A.; Palmieri, P.; Pitzer, R.; Rauhut, G.; Schütz, M.; Schumann, U.; Stoll, H.; Stone, A. J.; Tarroni, R.; Thorsteinsson, T.; Werner, H.-J.

(25) Hobza, P.; Selzle, H. L.; Schlag, E. W. *J. Phys. Chem.* **1996**, *100*, 18790−18794.

(26) Beran, G. J. O.; Head-Gordon, M.; Gwaltney, S. R. *J. Chem. Phys.* **2006**, *124*, 114107.

(27) Jensen, F. *Chem. Phys. Lett.* **1996**, *261*, 633−636.

(28) van Mourik, T.; Karamertzanis, P. G.; Price, S. L. *J. Phys. Chem. A* **2006**, *110*, 8−12.

(29) Scott, A. P.; Radom, L. *J. Phys. Chem.* **1996**, *100*, 16502−16513.

(30) Hunig, I.; Kleinermanns, K. *Phys. Chem. Chem. Phys.* **2004**, *6*, 2650−2658.

(31) Dian, B. C.; Longarte, A.; Zwier, T. S. *J. Chem. Phys.* **2003**, *118*, 2696−2706.

(32) Brauer, B.; Gerber, R. B.; Kabeláč, M.; Hobza, P.; Bakker, J. M.; Abo Riziq, A.; de Vries, M. S. *J. Phys. Chem. A* **2005**, *109*, 6974−6984.

(33) Godfrey, P. D.; Brown, R. D. *J. Am. Chem. Soc.* **1998**, *120*, 10724−10732.